Journal of Marine Science and Technology (2021) 26:734–749
https://doi.org/10.1007/s00773-020-00766-x

ORIGINAL ARTICLE

Underwater acoustic positioning based on the robust zero-difference Kalman filter

Junting Wang[1] · Tianhe Xu[1] · Bingsheng Zhang[2] · Wenfeng Nie[1]

Received: 9 March 2020 / Accepted: 5 September 2020 / Published online: 18 September 2020
© The Japan Society of Naval Architects and Ocean Engineers (JASNAOE) 2020

Abstract
The accuracy of underwater acoustic positioning is greatly influenced by both systematic error and gross error. Aiming at these problems, the paper proposes a robust zero-difference Kalman filter based on the random walk model and the equivalent gain matrix. The proposed algorithm takes systematic error as a random walk process, and estimates it together with the position parameters by using zero-difference Kalman filter. In addition, the equivalent gain matrix based on the robust estimation of Huber function is constructed to resist the influence of gross error. The proposed algorithm is verified by the simulation experiment and a real one for underwater acoustic positioning. The results demonstrate that the robust zero-difference Kalman filter can control both the effects of systematic error and gross error without amplifying the influence of the observation random noise, which is obviously superior to the zero-difference least squares (LS), the single-difference LS and zero-difference Kalman filter in underwater acoustic positioning.

Keywords Systematic error · Gross error · Kalman filter · Zero-difference positioning · Robust estimation

1 Introduction

With the development of the national marine strategy and the marine resource exploration, accurate ocean navigation and positioning technology are needed to obtain the high-precision, large-scale marine environmental information [1–3]. Sound waves, rather than electromagnetic waves or light waves, are mainly used to estimate the position of the underwater target. The reason is that sound waves can spread hundreds of kilometers in the water while electromagnetic waves and light waves decay quickly [4]. The classical acoustic-based approaches for underwater target positioning include long baseline (LBL), short baseline (SBL), ultra-short baseline (USBL) and underwater global positioning system (GPS) according to the acoustic baseline range [5, 6]. The shipborne acoustic positioning generally adopts the voyage positioning mode, which is affected by the geometric structure of trajectory and the measurement error related to the time delay as well as the sound speed [7, 8].

For underwater acoustic positioning, there inevitably exist the gross error, the random error and the systematic error caused by the marine environment and the observation instrument. Many studies have been dedicated to improve the underwater positioning model and the error correction method. Xu et al. [9] first proposed the underwater difference positioning algorithm including the single difference algorithm between the observation epochs and the double difference algorithm which can greatly improve the accuracy of seafloor deformation measurement. Zhao et al. [10] proposed a ship-board difference positioning method based on selecting weight iteration. Although the difference positioning algorithm can weaken the effects of the systematic errors, it enlarges the influence of random errors, which decreases the accuracy of the underwater acoustic positioning. Aiming at the time delay error, a positioning model considering the apparent time delay error as unknown parameter is proposed [11]. Yan et al. [12] proposed a long baseline positioning algorithm for moving buoy by estimating the uncertain sound speed as an unknown parameter. However, even though the time delay error or the unknown sound speed is estimated as a fixed systematic parameter, it is hard to be accurately estimated since it changes with the

✉ Tianhe Xu
thxu@sdu.edu.cn

1 Institute of Space Science, Shandong University, Weihai, China

2 College of Geology Engineering and Geomantic, Chang'an University, Xi'an, Shanxi, China

change of the marine environment. In the global navigation satellite system (GNSS) positioning, Paziewski and Wielgosz [13] used the random walk model to estimate the inter-system biases as the unknown parameters, which inspires us to apply this method to estimate the systematic error in underwater acoustic positioning. As for gross errors, Zhou [14] proposed the IGG robust estimation method based on the equivalence weight. On this basis, Yang et al. [15] developed the bi-factor equivalence weight based on the robust estimation for correlation observation. Xu et al. [16] proposed a robust estimation method based on the symbol constraint. Wang et al. [17] proposed a robust extended Kalman filter using W-test statistics based on filtering residuals to eliminate the effect of gross errors on GNSS navigation solutions. Yang et al. [18] proposed the robust M–M unscented Kalman filtering for GPS/IMU navigation. The applications of the robust estimation in GPS navigation and positioning have been widely adopted and tested [19]. Wang et al. [20] proposed an adaptive robust unscented Kalman filter for autonomous underwater vehicle (AUV) acoustic navigation, which constructs the judgment factor and adaptive factor by the prediction residual to balance the contribution between the observation information and AUV motion state information.

The zero-difference (ZD) least squares (LS) is rarely adopted for the high precision underwater positioning due to the effects of systematic error as well as gross error. At the same time, the single-difference (SD) LS of adjacent epoch enlarges the influence of random errors and even the gross errors while it suppresses the effects of systematic errors. To solve the aforementioned problems, this paper proposes a robust zero-difference Kalman filter based on the random walk model and the equivalent gain matrix to resist the effects of systematic errors and gross errors in underwater acoustic positioning. The proposed method involves a robust estimation method based on the prediction residual as well as the observation variance, and an improved KF with systematic error compensation, which has obvious differences compared to the method of reference [20].

The paper is organized as follows. We firstly present an improved zero-difference positioning function model as well as the zero-difference Kalman filter by estimating the systematic error as the random walk process in Sect. 2. Then Sect. 3 introduces the theoretical derivation and algorithm implementation of the robust zero-difference Kalman filter. The robust zero-difference Kalman filter is verified and analyzed by the simulation experiment and a real one for underwater acoustic positioning in Sect. 4. Finally, we summarize the significant conclusions in Sect. 5.

2 Method

2.1 Zero-difference positioning function model

The transducer under the survey ship can continuously send sound waves to the transponder to get the signal propagation time [21]; therefore, the range between the transducer and the transponder at the different time and position can be obtained by the travel time and the sound speed structure [22].

As shown in Fig. 1, assuming that the transducer at position $\mathbf{X}_k$ and time t_k transmits an acoustic signal to the transponder to get the slant range ρ_k, the transponder coordinates can be obtained through the intersection positioning method, which can be regarded as a prototype of the underwater zero-difference positioning, since there are no differential operations on observations between epochs and transponder stations. The observation model of underwater zero-difference positioning can be expressed as

$$\rho_k = f\left(\mathbf{X}_k, \mathbf{X}_o\right) + \delta\rho_{d_k} + \delta\rho_{v_k} + \varepsilon_k, \tag{1}$$

$$f\left(\mathbf{X}_k, \mathbf{X}_o\right) = \sqrt{(x_k - x_o)^2 + (y_k - y_o)^2 + (z_k - z_o)^2}, \tag{2}$$

$$\rho_k = ct_k, \tag{3}$$

where $\mathbf{X}_o = (x_o, y_o, z_o)$ is the unknown position vector of the transponder, and $\mathbf{X}_k = (x_k, y_k, z_k)$ is the position vector of

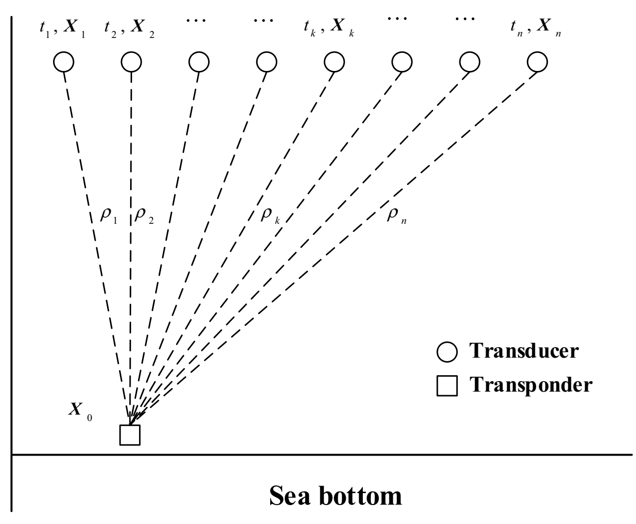

Fig. 1 The geometric diagram of underwater zero-difference positioning

transducer under the ship, which can be directly calculated from the kinematic GNSS. $f\left(\mathbf{X}_k, \mathbf{X}_o\right)$ is the theoretical range between the transponder and the transducer. $\delta\rho_{d_k}$ is the systematic error due to the time delay in re-transmitting the received signal from the transponder back to the transducer, $\delta\rho_{v_k}$ is the systematic error due to the spatial and temporal variation in the sound speed structure, ε_k is the random ranging error. t_k is the travel time between the transducer and the transponder, and c is the sound speed.

In the actual underwater acoustic positioning, the sound speed error is affected by the ocean internal wave and has a periodic variation. In addition, the systematic error related to time delay for the same transponder is approximately equal [23, 24]. Therefore, the systematic error related to the time delay and the sound speed can be estimated as an unknown parameter and the observation Eq. 1 can be rewritten as

$$\rho_k = f\left(\mathbf{X}_k, \mathbf{X}_o\right) + \delta\rho_k + \varepsilon_k, \tag{4}$$

where $\delta\rho_k$ is the estimated parameter of the systematic error.

Equation 4 is linearized as

$$\rho_k - f\left(\mathbf{X}_k, \mathbf{X}_o^0\right) - \delta\rho_k^0 = a_k d\mathbf{X}_o + d\delta\rho_k + \varepsilon_k + b_k\varepsilon_{\mathbf{X}_k}, \tag{5}$$

where $\mathbf{X}_o^0$, $\delta\rho_k^0$ are approximate values for $\mathbf{X}_o$ and $\delta\rho_k$. $d\mathbf{X}_o$ and $d\delta\rho_k$ are the unknown coordinate correction vector and the systematic error correction vector to be estimated with $\mathbf{X}_o = \mathbf{X}_o^0 + d\mathbf{X}_o$ and $\delta\rho_k = \delta\rho_k^0 + d\delta\rho_k$, respectively. a_k and b_k are the first-order partial derivatives with respect to $\mathbf{X}_o$ and $\mathbf{X}_k$, respectively, and $\varepsilon_{\mathbf{X}_k}$ is the random errors of the survey ship positions.

When combining all the measurements, the linear observation equation of underwater zero-difference positioning can be expressed as:

$$\mathbf{Z} = \mathbf{H}d\mathbf{X'}_o + \mathbf{V}, \tag{6}$$

$$\mathbf{H} = \begin{bmatrix} \frac{\partial f_1}{\partial x} & \frac{\partial f_1}{\partial y} & \frac{\partial f_1}{\partial z} & 1 \\ \frac{\partial f_2}{\partial x} & \frac{\partial f_2}{\partial y} & \frac{\partial f_2}{\partial z} & 1 \\ \frac{\partial f_3}{\partial x} & \frac{\partial f_3}{\partial y} & \frac{\partial f_3}{\partial z} & 1 \\ \vdots & \vdots & \vdots & \vdots \\ \frac{\partial f_n}{\partial x} & \frac{\partial f_n}{\partial y} & \frac{\partial f_n}{\partial z} & 1 \end{bmatrix}, \tag{7}$$

$$\mathbf{Z} = \begin{bmatrix} \rho_1 - f\left(\mathbf{X}_1, \mathbf{X}_o^0\right) - \delta\rho_1^0 \\ \rho_2 - f\left(\mathbf{X}_2, \mathbf{X}_o^0\right) - \delta\rho_2^0 \\ \rho_3 - f\left(\mathbf{X}_3, \mathbf{X}_o^0\right) - \delta\rho_3^0 \\ \vdots \\ \rho_n - f\left(\mathbf{X}_n, \mathbf{X}_o^0\right) - \delta\rho_n^0 \end{bmatrix}, \tag{8}$$

where $\mathbf{X'}_o = (x_o, y_o, z_o, \delta\rho_k)$, $\mathbf{Z}$ is the constant term, $\mathbf{H}$ is the coefficient matrix of observation equation, and $\mathbf{V}$ is the observation residual vector.

2.2 Zero-difference Kalman filter

The observation and state equations using zero-difference Kalman filter for underwater acoustic positioning can be expressed as [25]:

$$\mathbf{Z}_\mathrm{k} = \mathbf{H}_k d\mathbf{X'}_{o,k} + \mathbf{V}_k, \tag{9}$$

$$\mathbf{X'}_{o,k} = \boldsymbol{\varphi}_{k,k-1}\mathbf{X'}_{o,k-1} + \boldsymbol{\omega}_{k-1}, \tag{10}$$

where $\mathbf{X'}_{o,k} = (x_{o,k}, y_{o,k}, z_{o,k}, \delta\rho_k)$ denotes the estimated parameter vector of the transponder position and the systematic error at time t_k, $\mathbf{Z}_\mathrm{k}$ is the observation vector with covariance matrix $\mathbf{R}_k$, assumed to be white, $\mathbf{H}_k$ is the coefficient matrix of observation equation and $\mathbf{V}_k$ is the observation residual vector. $\boldsymbol{\varphi}_{k,k-1}$ is the state transition matrix from epoch t_{k-1} to t_k. $\boldsymbol{\omega}_{k-1}$ is the process noise vector with covariance matrix $\mathbf{Q}_k$, assumed to be white.

The discrete first-order Gauss–Markov process [26] describes the epoch state changes of related parameters, and the mathematical expression is as follows:

$$\begin{cases} \mathbf{X'}_{o,k} = e^{-\frac{\Delta t}{\tau}}\mathbf{X'}_{o,k-1} + \boldsymbol{\omega}_{k-1}, \quad \boldsymbol{\omega}_{k-1} = \int\limits_{t_{k-1}}^{t_k} e^{-\frac{\Delta t}{\tau}}\boldsymbol{\omega}dt \\ E(\boldsymbol{\omega}_k\boldsymbol{\omega}_{k-1}) = \frac{1}{2}\tau(1 - e^{-\frac{2\Delta t}{\tau}})\delta \end{cases}, \tag{11}$$

where $\Delta t = t_k - t_{k-1}$, τ is the time constant, and δ is Dirac function.

When $\tau \to \infty$, the state of Eq. 11 is the random walk process

$$\begin{cases} \mathbf{X'}_{o,k} = \mathbf{X'}_{o,k-1} + \boldsymbol{\omega}_{k-1} \\ E(\boldsymbol{\omega}_k\boldsymbol{\omega}_{k-1}) = \sigma_\mathbf{w}^2\delta \end{cases}. \tag{12}$$

When $\tau \to 0$, the state of Eq. 11 is the white noise

$$\begin{cases} \mathbf{X'}_{o,k} = \boldsymbol{\omega}_{k-1} \\ E(\boldsymbol{\omega}_k\boldsymbol{\omega}_{k-1}) = \sigma_\mathbf{w}^2\delta \end{cases}, \tag{13}$$

where $\sigma_\mathbf{w}^2$ is the variance of the state parameters.

The unknown parameters of the zero-difference Kalman filter are the transponder position and the systematic error. Since the transponder position parameters are constants and the systematic error parameter changes regularly with time, the state transition matrix and the state noise matrix of Eq. 10 are given by

$$\boldsymbol{\varphi}_{k,k-1} = \mathbf{I}_{4\times4}, \tag{14}$$

$$\mathbf{Q}_k = \begin{bmatrix} 0 & & & \\ & 0 & & \\ & & 0 & \\ & & & \sigma^2_{\omega_{\delta\rho}} \end{bmatrix}, \tag{15}$$

where $\mathbf{I}_{4\times4}$ is a unit array of four rows and four columns, and $\sigma^2_{\omega_{\delta\rho}}$ is the variance of the systematic error parameter.

The covariance propagation equation is given by

$$\mathbf{P}_{k,k-1} = \boldsymbol{\varphi}_{k,k-1}\mathbf{P}_{k-1}\boldsymbol{\varphi}^T_{k,k-1} + \mathbf{Q}_{k-1}. \tag{16}$$

The solutions for the estimated state vector, the Kalman filter gain matrix and the covariance matrix of the estimated state can be obtained as [25]

$$\mathbf{X}'_{o,k} = \mathbf{X}'_{o,k-1} + \mathbf{K}_k[\mathbf{Z}_k - \mathbf{H}_k d\mathbf{X}'_{o,k-1}], \tag{17}$$

$$\mathbf{K}_k = \mathbf{P}_{k,k-1}\mathbf{H}_k^T[\mathbf{H}_k\mathbf{P}_{k,k-1}\mathbf{H}_k^T + R_k]^{-1}, \tag{18}$$

$$\mathbf{P}_k = [\mathbf{I} - \mathbf{K}_k\mathbf{H}_k]\mathbf{P}_{k,k-1}. \tag{19}$$

3 Robust zero-difference Kalman filter

In underwater acoustic positioning, when the observation contains the gross error, the measurement equation should be

$$\rho_k = f\left(\mathbf{X}_k, \mathbf{X}_o\right) + \delta\rho_k + \mathbf{B}_k\boldsymbol{\Delta}_k + \varepsilon_k, \tag{20}$$

where $\mathbf{B}_k$ is the interference matrix of gross error, and $\boldsymbol{\Delta}_k$ is the gross error.

If the standard Kalman filter is still used for calculation, the prediction residual with the gross error is as follows:

$$\tilde{V}_k = \rho_k - f\left(\mathbf{X}_k, \mathbf{X}_o\right) - \delta\rho_k = V_k + \mathbf{B}_k\boldsymbol{\Delta}_k, \tag{21}$$

where V_k and $\tilde{V}_k$ are the prediction residual vector without the gross error and with the gross error respectively.

The gross error is fully reflected in the prediction residual, then the state vector is

$$\mathbf{X}'_k = \mathbf{X}'_{k,k-1} + \mathbf{K}_k\tilde{V}_k. \tag{22}$$

According to Eq. 22, the gross error in the observation affects the state vector $\mathbf{X}'_k$ through the gain matrix $\mathbf{K}_k$. To resist the influence of gross error, a robust zero-difference Kalman filter is adopted based on the equivalent gain matrix. By using the prediction residual and the observation variance to construct the judgment factor S_k, the gross error in the observation equation can be efficiently detected. Based on the idea of equivalent gain matrix [20] and equivalent weight function of Huber [27, 28], the equivalent gain matrix related to the constant k_0 is constructed to reduce the influence of gross error. The equivalent gain matrix is expressed as

$$\overline{\mathbf{K}}_k = \begin{cases} \mathbf{K}_k & |S_k| < k_0 \\ \mathbf{K}_k \dfrac{k_0}{|S_k|} & |S_k| \geq k_0 \end{cases}, \tag{23}$$

where k_0 is a constant, generally, $k_0 = 1 \sim 2$.

$$S_k = V_k / \sqrt{\mathbf{D}_{V(k)}}, \tag{24}$$

$$\mathbf{D}_{V(k)} = [\mathbf{I} - \mathbf{H}_k\mathbf{K}_k]R_k, \tag{25}$$

where V_k is the prediction residual vector, and $\mathbf{D}_{V(k)}$ is the covariance matrix of observation vector.

When there exists gross error in the observations, the corresponding $\overline{\mathbf{K}}_k$ will be decreased and the influence of gross error on KF will be reduced.

To resist the effects of both systematic error and gross error, a robust zero-difference Kalman filter based on the random walk model and the equivalent gain matrix is proposed. The flowchart of the proposed algorithm is shown in Fig. 2. The detailed steps of the algorithm are explained as follows:

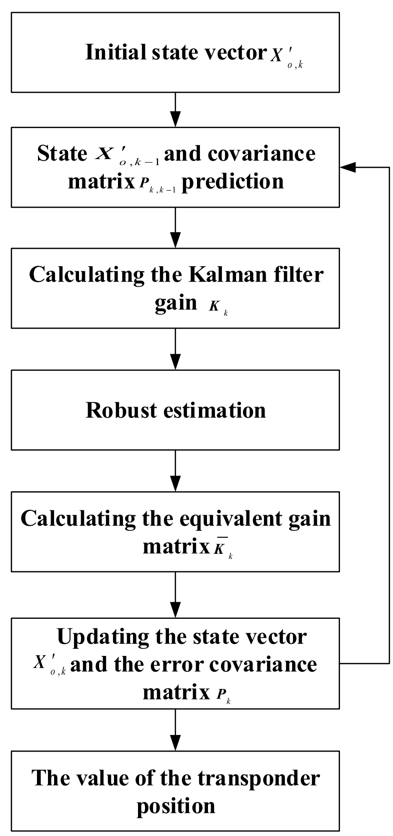

Fig. 2 The flowchart of the robust zero-difference Kalman filter

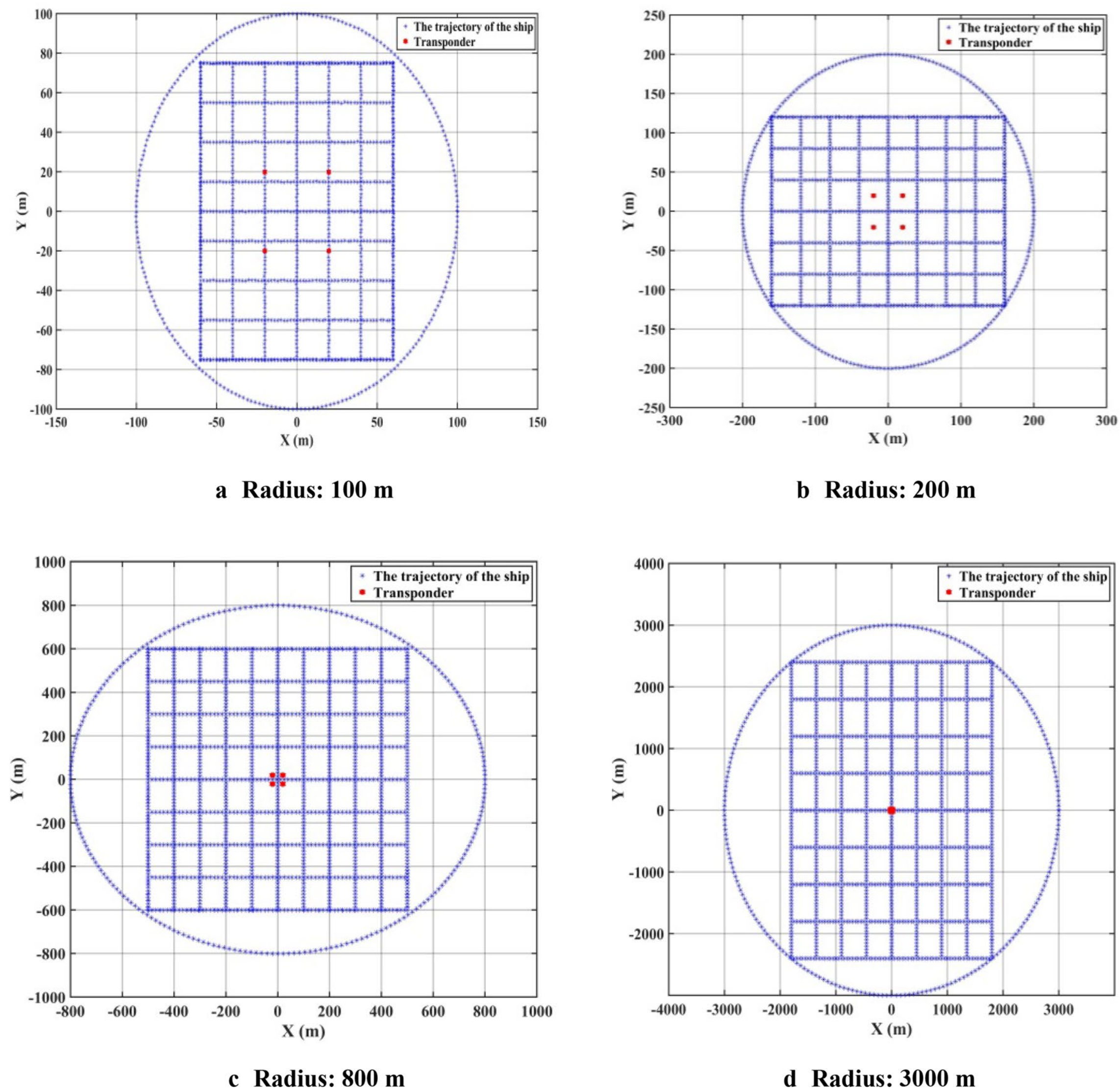

Fig. 3 The diagram of simulated ship and transponder

1. The initial state vector $\mathbf{X'}_{o,1} = (x_{o,1}, y_{o,1}, z_{o,1}, \delta\rho_1)$ including the transducer position and the systematic error is given.
2. The state vector $\mathbf{X'}_{o,k}$ and the corresponding covariance matrix $\mathbf{P}_{k,k-1}$ are calculated by Eqs. 10 and 16.
3. The gain matrix of the Kalman filter $\mathbf{K}_\mathrm{k}$ is computed by Eq. 18. The equivalent gain matrix $\overline{\mathbf{K}}_k$ based on robust estimation is calculated by Eq. 23.
4. The state vector and the error covariance matrix are estimated by Eqs. 26 and 27.

$$\mathbf{X'}_{o,k} = \mathbf{X'}_{o,k-1} + \overline{\mathbf{K}}_k [Z_k - \mathbf{H}_k d\mathbf{X'}_{o,k-1}], \tag{26}$$

$$\mathbf{P}_k = [\mathbf{I} - \overline{\mathbf{K}}_k \mathbf{H}_k] \mathbf{P}_{k,k-1}. \tag{27}$$

5. The steps (2)–(4) are repeated until filter convergence.

4 Simulation and real experimental analysis

4.1 Simulation analysis

Simulation analysis on the acoustic positioning based on the proposed method is conducted in this paper. As shown in Fig. 3, the four transponders are located at the positions of the asterisk symbol with the different underwater depth of 30 m, 100 m, 500 m and 3000 m. The trajectories of the ship are circles with the radius of 100 m, 200 m, 800 m and 3000 m as well as the linear track with the grid shape. The sampling interval is 2 s and the speed of the survey ship is

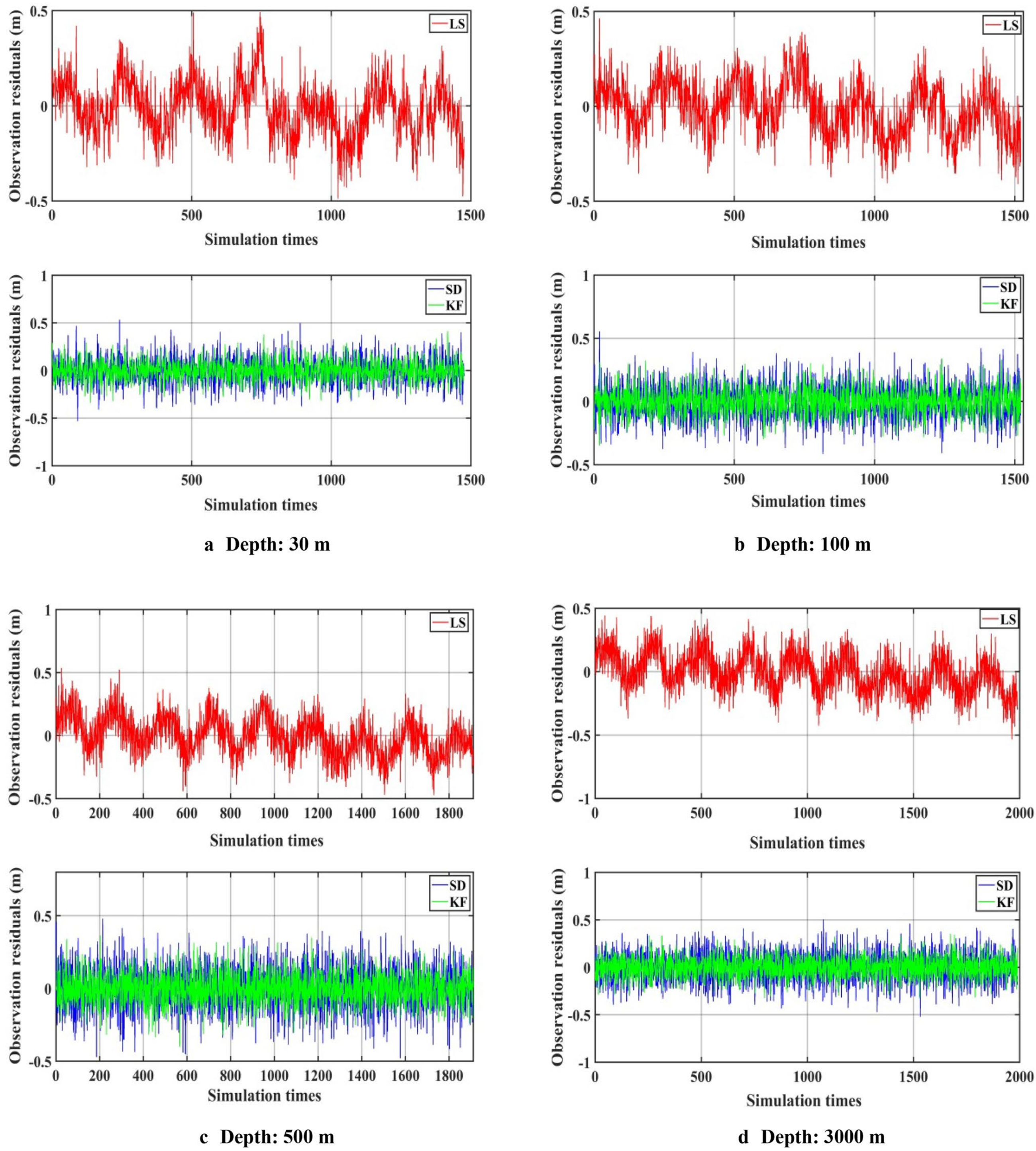

Fig. 4 The observation residuals of LS, SD and KF at different depths

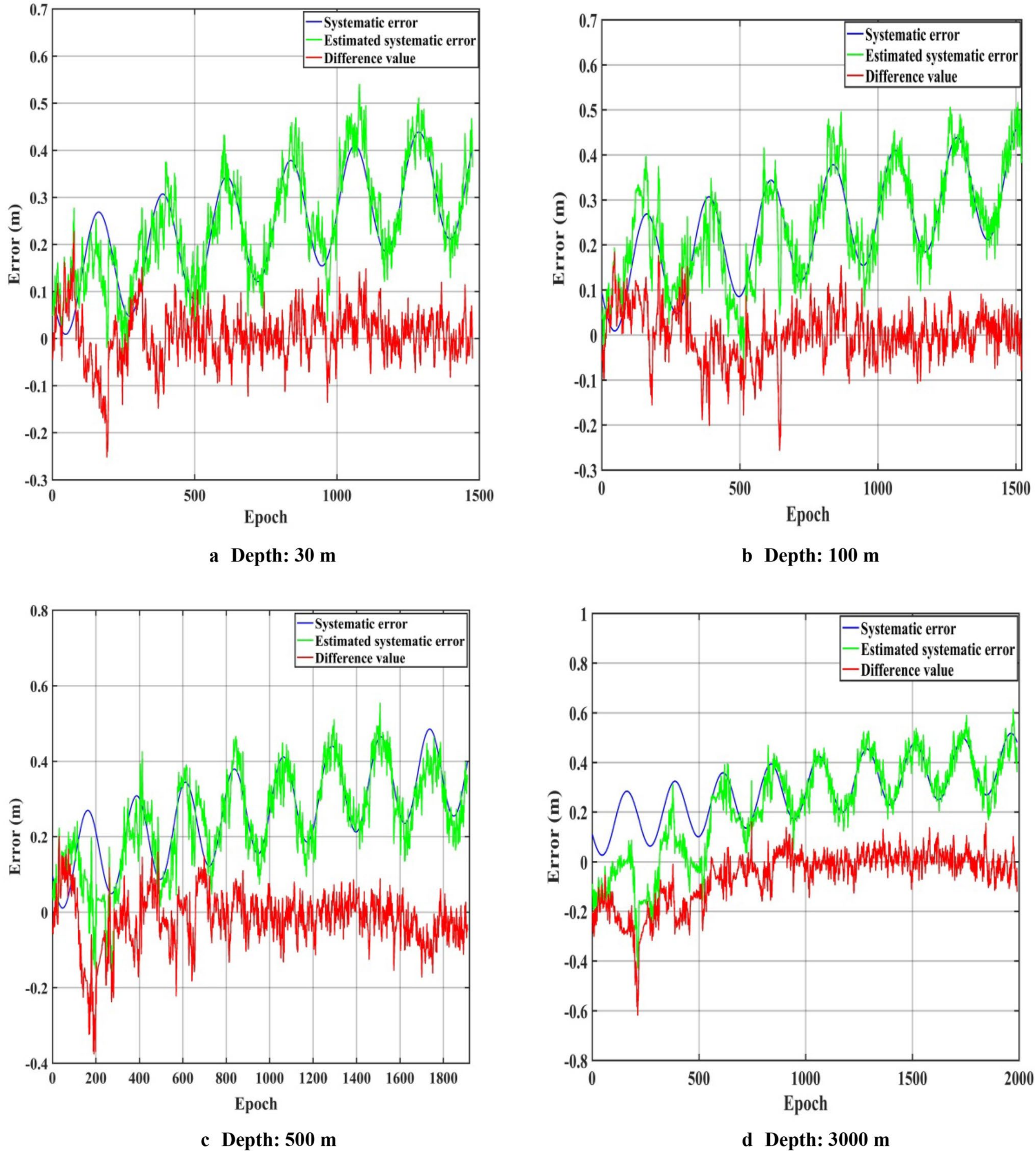

Fig. 5 The results of the estimated systematic errors by KF at different depths

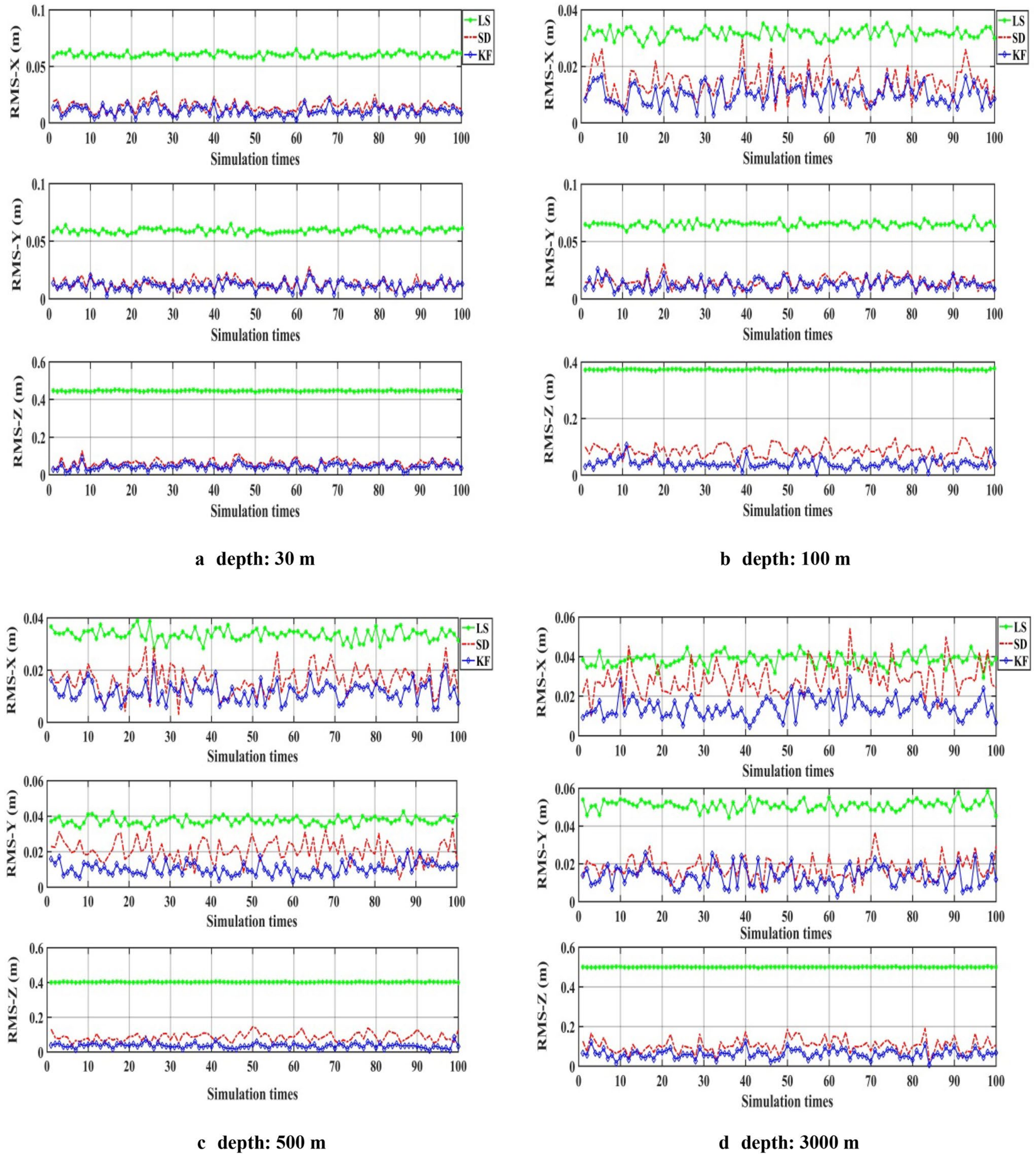

Fig. 6 The underwater positioning results of different algorithms at different depths

Table 1 The positioning result statistics of different algorithms

Depth (m)	Method	Mean RMS-X (m)	Mean RMS-Y (m)	Mean RMS-Z (m)	3D-RMS (m)
30	LS	0.061	0.059	0.447	0.455
	SD	0.014	0.013	0.062	0.065
	KF	0.011	0.012	0.045	0.048
100	LS	0.032	0.065	0.373	0.380
	SD	0.014	0.015	0.084	0.087
	KF	0.010	0.013	0.041	0.044
500	LS	0.034	0.038	0.403	0.406
	SD	0.016	0.020	0.086	0.090
	KF	0.012	0.011	0.036	0.040
3000	LS	0.039	0.051	0.500	0.504
	SD	0.029	0.018	0.105	0.110
	KF	0.014	0.014	0.062	0.065

about 1 m/s. The measured sound speed profile of 3000 m is adopted for the calculation of sound speed. The layered ray acoustic tracking algorithm is used to simulate the travel time, and the systematic error [29] is simulated based on Eq. 28 proposed in Xu et al. [9]. The slant range error caused by the random error is 0.1 m; therefore, the initial measurement noise variance is $R = 0.01\,\mathrm{m}^2$. The initial system noise matrix is $\mathbf{Q} = \mathrm{diag}[0 \;\; 0 \;\; 0 \;\; 0.001]\,\mathrm{m}^2$.

$$\delta\rho_{\mathrm{v}} = c_1 + c_2 \sin\left(\frac{2(t-t_0)}{T_S}\pi\right) + c_3 \sin\left(\frac{(t-t_0)}{T_L}\pi\right) + c_4\left[1 - \exp\left\{-\frac{1}{2}\|\mathbf{X}_o - \mathbf{X}\|/(2\mathrm{km})^2\right\}\right], \tag{28}$$

where the constant term is $c_1 = 0.1$ m, the short-period internal wave error term is $c_2 = 0.12$ m, the long-period error term is $c_3 = 0.3$ m, the term related to the measurement range is $c_4 = 0.02$ m, the short period of internal wave is $T_S = 15 * 60$ s (equal to 15 min) and the long period of internal wave is $T_L = 12 * 3600$ s (equal to 12 h). $\|\mathbf{X}_o - \mathbf{X}\|$ is the distance between the transducer and the transponder.

The zero-difference least squares (LS), the single-difference least squares (SD), the zero-difference Kalman filter (KF), the robust zero-difference least squares(R-LS), the robust single difference least squares (R-SD) and the robust zero-difference Kalman filter (R-KF) are conducted and compared for underwater acoustic positioning. Firstly, the proposed algorithm is validated in the case without gross error. The observation residuals of LS, SD and KF as well as the estimated systematic errors by KF are shown in Figs. 4 and 5. Monte Carlo experimental simulation with 100 times is conducted, the root mean squares (RMS) of the transponder position calculated at the different depth and the different algorithm is shown in the Fig. 6. In calculating the formula of RMS, $X_{o,k}$ and $\hat{X}_{o,k}$ are the calculation value and the real value of the transponder respectively. N is the number of the transponder.

As shown in Figs. 4 and 5, the SD can effectively reduce the effects of systematic errors compared with the LS. However, the SD produces larger random errors compared with the KF. The KF can effectively estimate systematic error parameters, together with position parameter without enlarging the influence of random errors. Therefore, the KF can significantly improve the underwater positioning accuracy.

As shown in Fig. 6 and Table 1, when there exist random errors, systematic errors and no gross errors in the acoustic observations, the LS cannot resist the effects of the systematic errors on the positioning result, especially in the Z direction of coordinates. The SD and KF can both reduce the influence of the systematic errors and greatly improve the positioning accuracy. For the case of underwater 30 m depth, the three-dimension (3D) RMSs of SD and KF are 0.065 m and 0.048 m, respectively, compared to LSs 0.455 m, with the improvement of 85.7% and 89.4%. For the case of 100 m depth, they are 0.087 m and 0.044 m, respectively, compared to LSs 0.380 m, with the improvement of 77.1% and 88.4%. For the case of 500 m depth, they are 0.090 m and 0.040 m, respectively, compared to LSs 0.406 m, with the improvement of 77.8% and 90.1%. For the case of 3000 m depth, they are 0.110 m and 0.065 m, respectively, compared to LSs 0.504 m, with the improvement of 78.2% and 87.1%. In addition, the KF can further enhance the positioning accuracy with about 5–12% improvement compared to the SD.

Secondly, to further verify the performance of LS, SD and KF in the case of the ship trajectories with irregular curve, the transponders with the different underwater depth of 30 m, 100 m, 500 m and 3000 m are positioned by the simulated trajectories as shown in Fig. 7. Table 2 presents the RMSs of different algorithms and depths. For the case of underwater 30 m depth, the 3D RMSs of SD and KF are 0.079 m and 0.057 m compared to the 0.362 m of LS, with the improvement of 78.2% and 84.3%. For the case of 100 m depth, they are 0.175 m and 0.082 m compared to the 0.304 m of LS, with the improvement of 42.4% and 73.0%. For the case of 500 m depth, they are 0.127 m and 0.061 m compared to the 0.373 m of LS, with the improvement of 66.0% and 83.6%. For the case of 3000 m depth, they are 0.223 m and 0.165 m compared to the 0.442 m of LS, with the improvement of 47.3% and 62.7%. Therefore, the performance of KF is also better than that of LS and SD in the case of the ship trajectories with irregular curve.

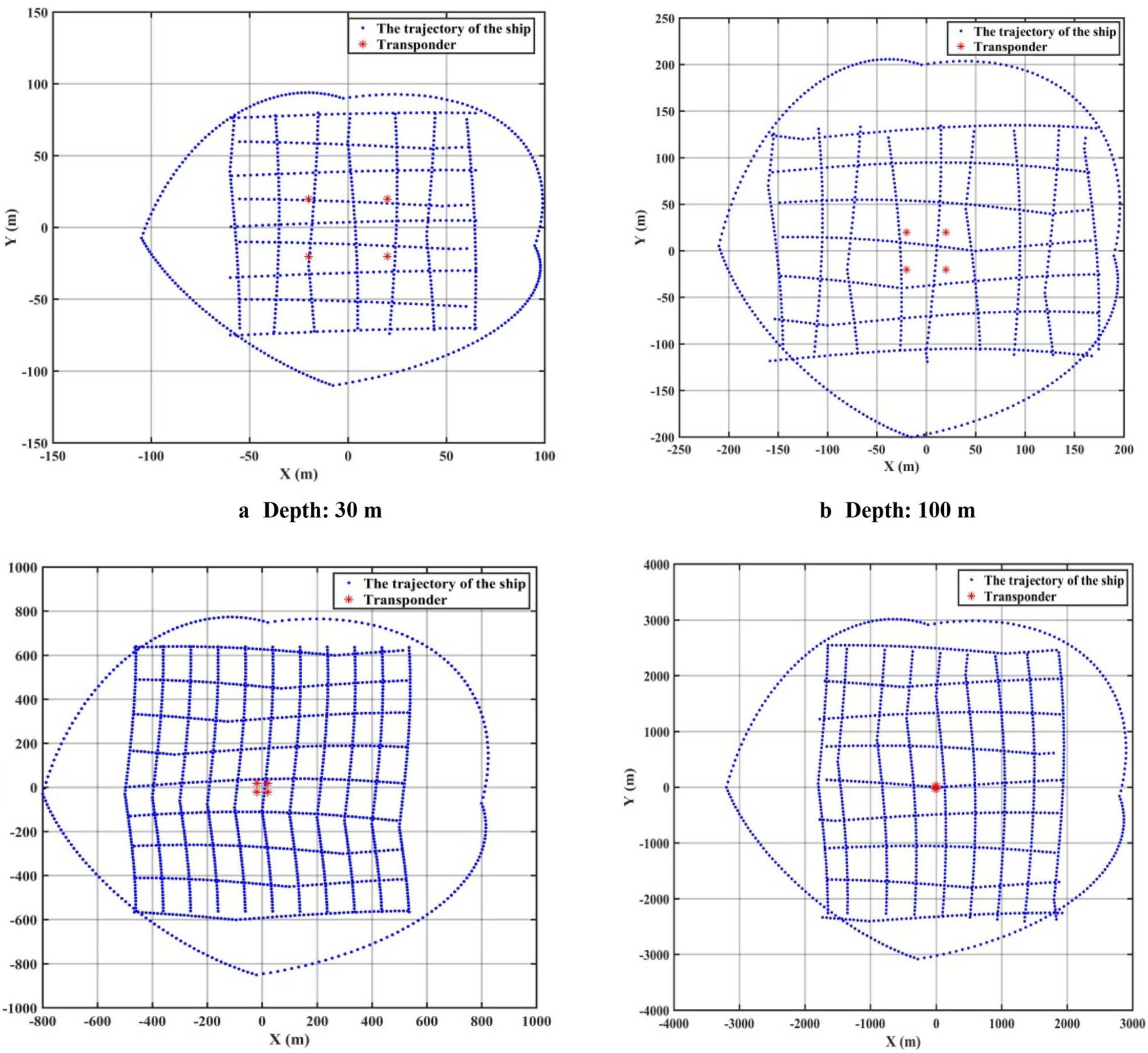

a Depth: 30 m **b Depth: 100 m**

c Depth: 500 m **d Depth: 3000 m**

Fig. 7 The diagram of the simulated ship and transponder in different depths

Finally, the time delay observation is added to the gross errors based on normal distribution with zero mean and standard deviation of 0.05 s, and the gross errors are added in the acoustic observations every 50 s. Figure 8 shows the result of the estimated systematic error by the R-KF. At the same time, the positioning results of the non-robust estimation and the robust estimation are shown in Figs. 9, 10, 11 and 12.

Figure 8 shows that the R-KF can resist the influence of gross errors on the position and systematic error parameter based on the equivalent gain matrix. As shown in the Figs. 9, 10, 11 and 12, the accuracy of the SD is significantly reduced compared with the LS and the KF due to the effects of the gross errors. The R-SD can also resist the influences of the gross errors by the robust estimation and reduce the influence of the systematic errors to improve the accuracy of the underwater positioning compared with the R-LS. However, the R-SD has also the disadvantage of enlarging the effects of random errors, which leads to the positioning accuracy lower than that of the R-KF. The R-KF can estimate the systematic errors by the random walk process without enlarging the influence of the random errors, and provide robust solutions by using the equivalent gain matrix, which has higher precision and stability than those of the other two algorithms.

Table 2 The positioning result statistics of different algorithms

Depth (m)	Method	Mean RMS-X (m)	Mean RMS-Y (m)	Mean RMS-Z (m)	3D-RMS (m)
30	LS	0.047	0.066	0.353	0.362
	SD	0.020	0.017	0.074	0.079
	KF	0.015	0.013	0.054	0.057
100	LS	0.022	0.045	0.299	0.304
	SD	0.021	0.019	0.172	0.175
	KF	0.014	0.014	0.079	0.082
500	LS	0.037	0.037	0.369	0.373
	SD	0.027	0.023	0.122	0.127
	KF	0.019	0.012	0.056	0.061
3000	LS	0.039	0.049	0.437	0.442
	SD	0.023	0.017	0.221	0.223
	KF	0.018	0.014	0.163	0.165

The means of RMS for 100 times of each algorithm are shown in Table 3. From Table 3, it can be seen that the positioning accuracy of the LS, SD and KF is greatly decreased by gross errors, especially for the SD due to the enlarged gross errors. R-LS, R-SD and R-KF can obviously improve the positioning by using robust estimation to resist the influence of the gross errors. For the case of underwater 30 m depth, the three-dimension (3D) RMSs of R-SD and R-KF are 0.076 m and 0.045 m, respectively, compared to R-LSs 0.463 m, with the improvement of 83.5% and 90.3%. For the case of 100 m depth, they are 0.103 m and 0.051 m, respectively, compared to LSs 0.378 m, with the improvement of 72.7% and 86.5%. For the case of 500 m depth, they are 0.099 m and 0.040 m, respectively, compared to LSs 0.406 m, with the improvement of 75.6% and 90.1%. For the case of 3000 m depth, they are 0.137 m and 0.062 m, respectively, compared to LSs 0.504 m, with the improvement of 72.8% and 87.7%. In addition, the R-KF can further enhance the positioning accuracy with about 7–15% improvement compared to R-SD.

4.2 Real experiment analysis

The in situ data were collected from an experiment conducted at Lingshan Island in Dec. 2017. Lingshan Island is located in Qingdao City, Shandong Province in China with longitude and latitude about 120° 13′ 02″ E, and 35° 46′ 53″ N, respectively. The single transponder is located at the ocean bottom, and the trajectory of the voyage move is centered around the transponder with a radius of about 50 m. The ultrashort baseline response mode is used for underwater positioning, and GPS receiver, attitude sensor and sound velocity profiler are auxiliary installed.

After preprocessing the measured data, LS, SD, KF, R-LS, R-SD and R-KF are used for the positioning calculation and then compared. The observation noise and the system noise of Kalman filter are set as $R = 1\ \mathrm{m}^2$ and $Q = \mathrm{diag}[0\ \ 0\ 0\ 0.001]\ \mathrm{m}^2$, respectively. Since the position of the underwater transponder in the experimental area is unknown, the positioning accuracy cannot be directly evaluated. To verify the accuracy of the algorithm, as shown in Fig. 13, the observations that are not involved in positioning calculation on the trajectory are selected to calculate the residuals, namely the observation ranges minus computation/theory ranges (O–C).

As shown in Table 4, the RMS of the validated residuals of the SD is lower than that of the LS and the KF. The reason may be that: (1) since the experiment is conducted in shallow sea, the influence of the systematic errors is relatively small; (2) the systematic error between the adjacent epochs are not exactly equal in the actual observations, and the SD cannot totally eliminate the systematic errors; (3) SD enlarges the influence of random errors. When using robust estimation, all the RMSs of the three methods decrease, which indicates that robust estimation can efficiently control the influence of gross errors. Compared with the R-LS and the R-SD, the RMS of the validated residuals of the R-KF is greatly reduced from 1.63 m and 1.81 m, respectively, to 0.85 m, which proves the higher precision of R-KF. From Fig. 14, it can be seen that both the KF and the R-KF need some certain epochs to make the filtering solution convergence. There is a bias between the solutions of R-KF and KF, since the former uses robust estimation to reduce the influence of the gross errors on the systematic error parameter, while the latter has no action on gross errors and inevitably brings the deviation of solution for underwater positioning.

5 Conclusion

To reduce the effects of the systematic error and the gross error on the underwater positioning, this paper proposes a robust zero-difference Kalman filter based on the random walk model and the equivalent gain matrix. After the validation from the simulation experiment and a real example, the following conclusions can be drawn.

1. Compared with the zero-difference LS, the single-difference LS between the observation epochs can reduce the influence of the systematic error. However, it also enlarges the influence of the random errors and the gross errors. Although the robust single-difference LS can eliminate the influence of the gross errors by the robust estimation, its accuracy of underwater position-

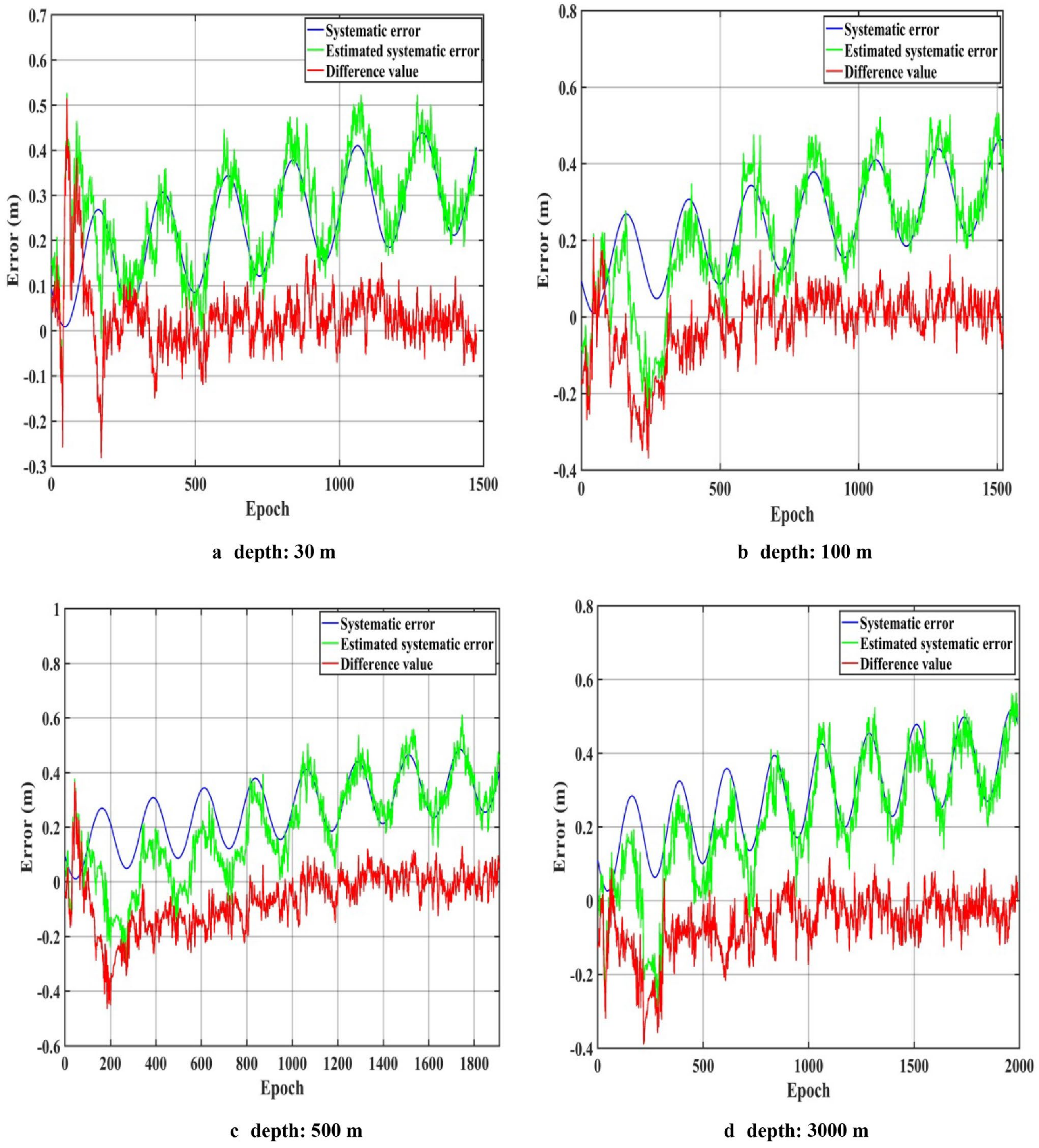

a depth: 30 m

b depth: 100 m

c depth: 500 m

d depth: 3000 m

Fig. 8 The results of the estimated systematic errors by R-KF at different depths

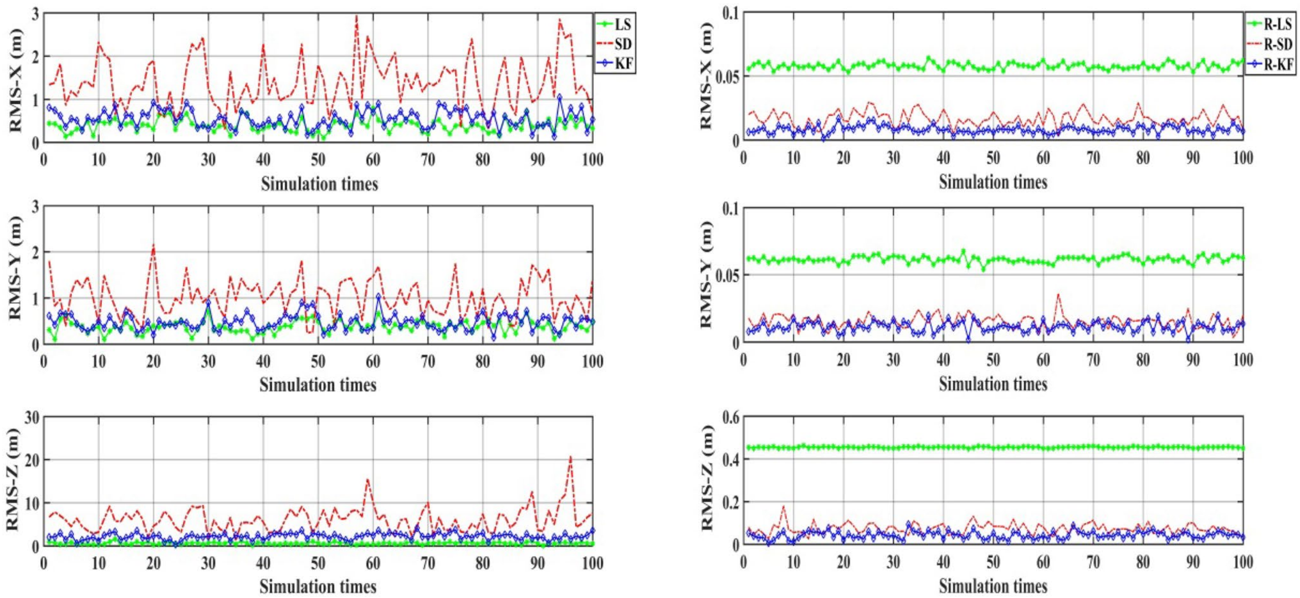

a **The non-robust estimation of the different algorithm** **b** **The robust estimation of the different algorithm**

Fig. 9 The positioning results at the depth of underwater 30 m

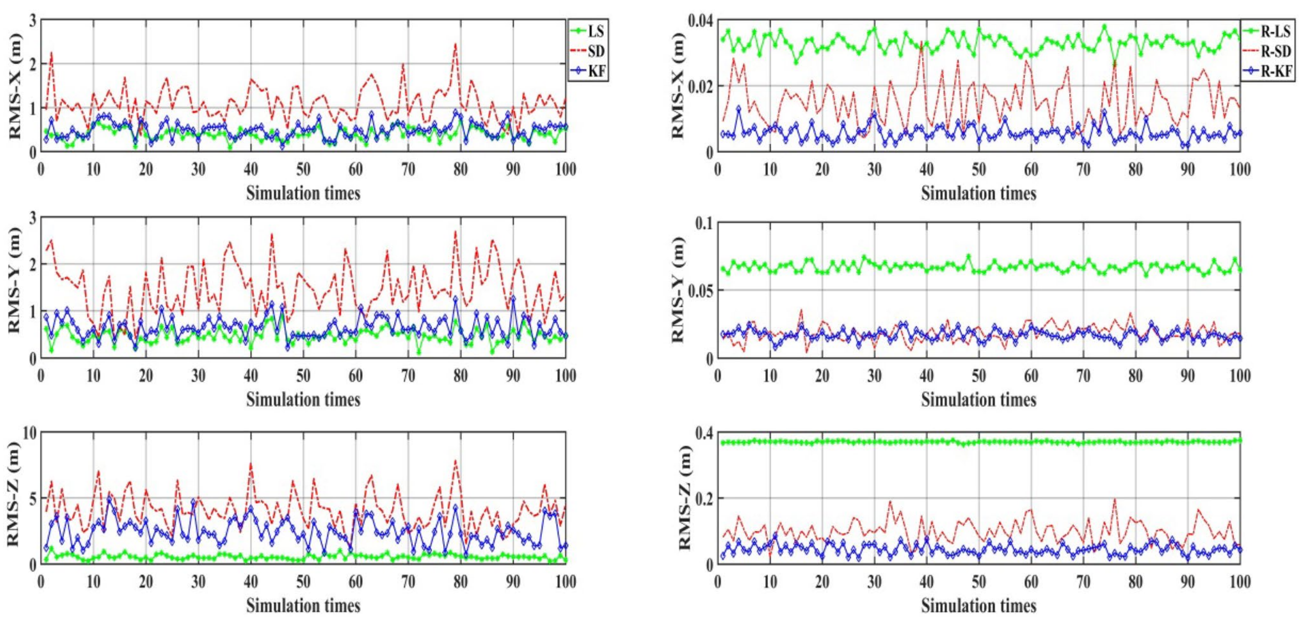

a **The non-robust estimation of the different algorithm** **b** **The robust estimation of the different algorithm**

Fig. 10 The positioning results at the depth of underwater 100 m

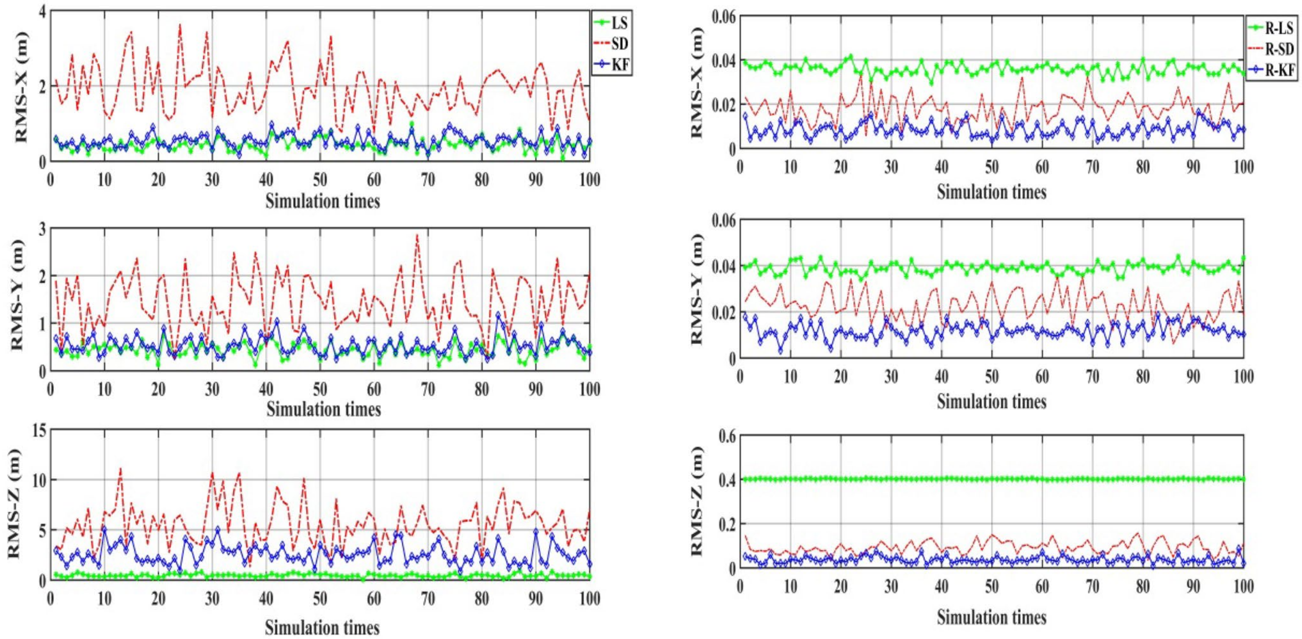

a The non-robust estimation of the different algorithm

b The robust estimation of the different algorithm

Fig. 11 The positioning results at the depth of underwater 500 m

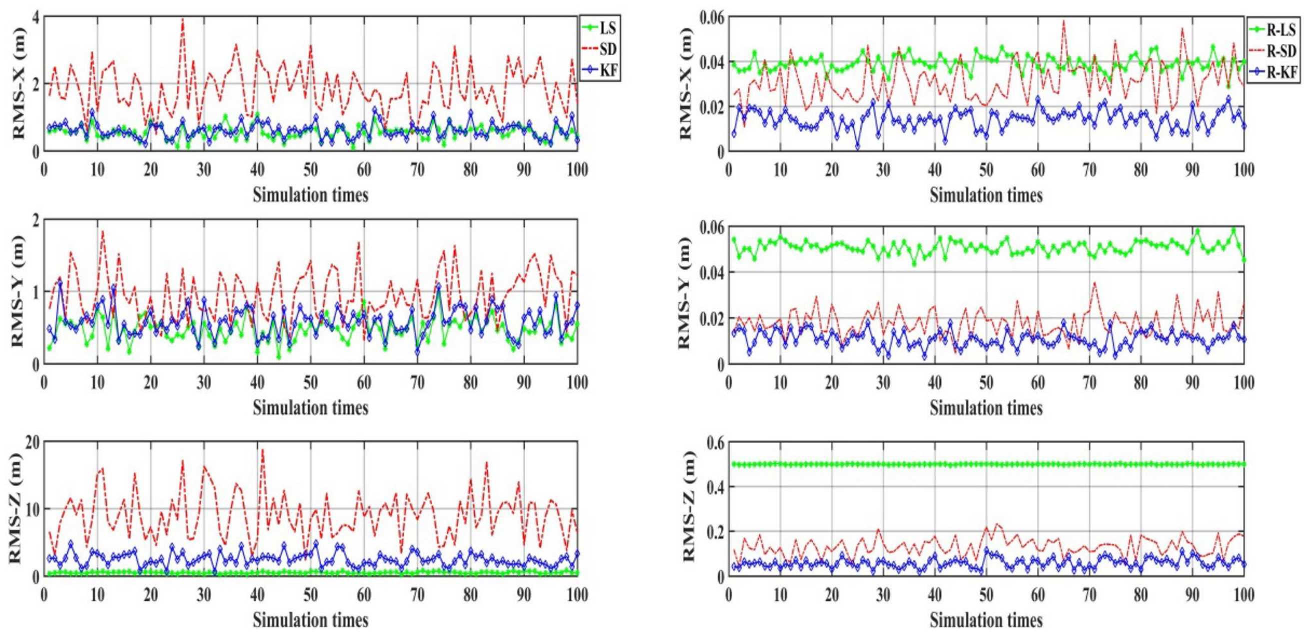

a The non-robust estimation of the different algorithm

b The robust estimation of the different algorithm

Fig. 12 The positioning results at the depth of underwater 3000 m

ing is greatly reduced by the enlarged random errors and the remained systematic errors. The accuracy of zero-difference Kalman filter can be significantly improved compared to the zero-difference LS and the single-difference LS. At the same time, the zero-difference Kalman filter has the better performance in the case of the ship trajectories with irregular curve.

2. The proposed robust zero-difference Kalman filter can estimate the systematic error by the random walk model without enlarging the influence of the random

Table 3 The positioning result statistics of different algorithms

Depth (m)	Method	Mean RMS-X (m)	Mean RMS-Y (m)	Mean RMS-Z (m)	3D RMS (m)
30	LS	0.399	0.382	0.662	0.862
	SD	1.382	1.013	6.183	6.416
	KF	0.554	0.480	2.249	2.365
	R-LS	0.058	0.062	0.455	0.463
	R-SD	0.017	0.015	0.073	0.076
	R-KF	0.008	0.011	0.043	0.045
100	LS	0.400	0.467	0.562	0.833
	SD	1.099	1.463	4.077	4.469
	KF	0.491	0.652	2.463	2.595
	R-LS	0.033	0.067	0.370	0.378
	R-SD	0.015	0.018	0.100	0.103
	R-KF	0.007	0.017	0.048	0.051
500	LS	0.442	0.442	0.490	0.794
	SD	1.920	1.458	5.563	6.063
	KF	0.547	0.543	2.588	2.600
	R-LS	0.036	0.039	0.402	0.406
	R-SD	0.018	0.027	0.093	0.099
	R-KF	0.008	0.011	0.038	0.040
3000	LS	0.554	0.477	0.558	0.920
	SD	1.892	0.138	12.070	12.218
	KF	0.617	0.584	2.511	2.651
	R-LS	0.039	0.051	0.500	0.504
	R-SD	0.031	0.018	0.133	0.137
	R-KF	0.014	0.011	0.059	0.062

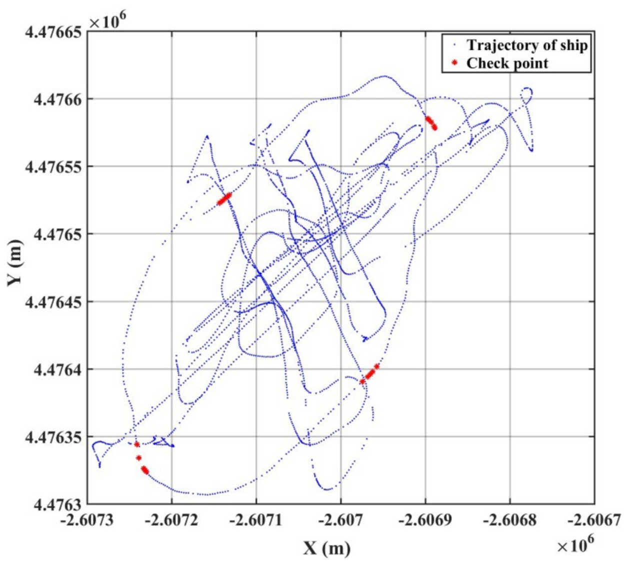

Fig. 13 The trajectory of ship and checkpoint

Table 4 The residuals statistics of the 20 epochs

Method	RMS (m)	Max (m)	Min (m)
LS	1.73	2.16	0.99
SD	1.91	2.59	1.39
KF	1.24	2.12	0.51
R-LS	1.63	2.17	0.92
R-SD	1.81	2.55	1.26
R-KF	0.85	1.69	0.04

errors, and resist the influence of the gross error by the equivalent gain matrix. In the simulating experiment, the positioning accuracy of the proposed algorithm is obviously superior to that of robust zero-difference LS and robust single-difference LS with the improvement of about 86–90% and about 5–15%, respectively. In the real data experiment, the RMS of the validated residuals of the robust zero-difference Kalman filter

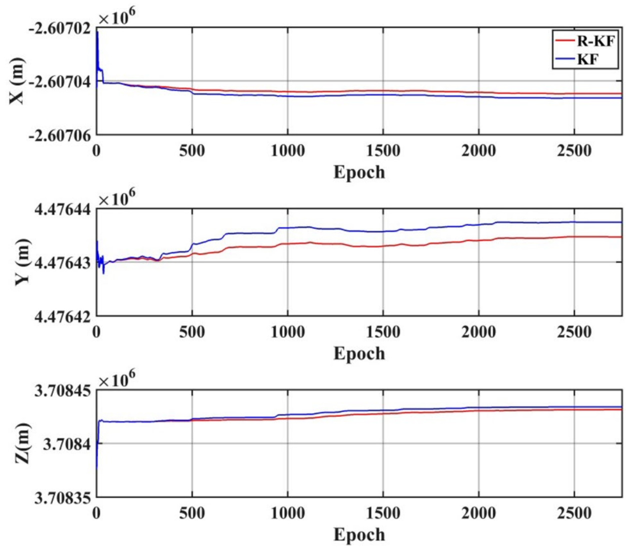

Fig. 14 The positioning result of epoch by epoch (blue line represents KF and red line is R-KF)

is about 0.8 m, and obviously less than that of robust zero-difference LS and the robust single-difference LS, which proves that the proposed algorithm has higher accuracy and stability.

Acknowledgements The study was funded by National Key Research and Development Program of China (2016YFB0501701), National Natural Science Foundation of China (41931076, 41874032 and 41731069).

References

1. Yoerger DR, Jakuba MV, Bradley AM et al (2007) Techniques for deep sea near bottom survey using an autonomous underwater vehicle[J]. Int J Robot Res 26(1):41–54
2. Stutters L, Liu H, Tiltman C et al (2008) Navigation technologies for autonomous underwater vehicles[J]. IEEE Trans Syst Man Cybernet Part C (Applications and Reviews) 38(4):581–589
3. Yang Y, Xu T, Xue S (2018) Progresses and prospects in developing marine geodetic datum and marine navigation of China[J]. J Geodesy Geoinf Sci 1(1):17–25
4. Frankenthal S (1984) Beam-intensity calculations with uncertain sound speed profiles[J]. J Acoust Soc Am 76(1):198–204
5. Leonard J, Bennett AA, Smith CM, Feder HJS (1998) Autonomous underwater vehicle navigation. MIT Marine Robotics Laboratory Technical memorandum 98–1
6. Erol-Kantarci M, Mouftah HT, Oktug S (2011) Localization techniques for underwater acoustic sensor networks[J]. IEEE Commun Surv Tut 13(3):487–502
7. Averbakh VS, Bogolyubov BN, Dubovoi YA et al (2002) Application of hydroacoustic radiators for the generation of seismic waves[J]. Acoust Phys 48(2):121–127
8. Sun SB, Yu SN, Shi ZB, Fu J, Zhao CH (2018) A novel single-beacon navigation method for group AUVs based on SIMO model [J]. IEEE Access 99:1–1
9. Xu PL, Ando M, Tadokoro K (2005) Precise, three-dimensional seafloor geodetic deformation measurements using difference techniques[J]. Earth Planets Space 57:795–808
10. Zhao S, Wang ZJ, Wu SY et al (2017) A ship-board acoustic difference positioning method based on selection weight iteration[J]. Oil Geophys Prospect 52(6):1150–1155
11. Zhao JH, Zou YJ, Zhang HM et al (2016) A new method for absolute datum transfer in seafloor control network measurement[J]. J Mar Sci Technol 21(2):216–226
12. Yan WS, Wei C, Cui RX (2015) Moving long baseline positioning algorithm with uncertain sound speed[J]. J Mech Sci Technol 29(9):3995–4002
13. Paziewski J, Wielgosz P (2015) Accounting for Galileo–GPS inter-system biases in precise satellite positioning[J]. J Geodesy 89(1):81–93
14. Zhou JW (1989) Classical error theory and robust estimation[J]. J Surve Mapping 18(02):115–120
15. Yang Y, Song L, Xu T (2002) Robust estimator for correlated observations based on bifactor equivalent weights[J]. J Geodesy 76(6–7):353–358
16. Xu PL (2005) Sign-constrained robust least squares, subjective breakdown point and the effect of weights of observations on robustness[J]. J Geodesy 79(1–3):146–159
17. Wang J, Xu C, Wang J (2008) Applications of robust kalman filtering schemes in GNSS navigation. Proceedings of the International Symposium on GPS/GNSS. Yokohama, Japan, pp 308–316
18. Yang C, Shi WZ, Chen W (2019) Robust M-M unscented Kalman filtering for GPS/IMU navigation[J]. J Geodesy Geodynamics 93:1093–1194
19. Yang YX, He H, Xu G (2001) Adaptively robust filtering for kinematic geodetic positioning[J]. J Geodesy 75(2–3):109–116
20. Wang JT, Xu TH, Wang ZJ (2020) Adaptive robust unscented Kalman filter for AUV acoustic navigation[J]. Sensors 20(1):60. https://doi.org/10.3390/s20010060
21. Gagnon K, Chadwell CD, Norabuena E (2005) Measuring the onset of locking in the Peru-Chile trench with GPS and acoustic measurements[J]. Nature 434(7030):205–208
22. Chadwell CD (2003) Shipboard towers for Global Positioning System antennas[J]. Ocean Eng 30(12):1467–1487
23. Spiess FN, Chadwell CD, Hildebrand JA et al (1998) Precise GPS/Acoustic positioning of seafloor reference points for tectonic studies[J]. Phys Earth Planet Interiors 108(2):101–112
24. Yi CH, Ren WJ, Chai W (2009) Analysis on error of secondary acoustic positioning system[J]. Oil Geophys Prospect 44(2):136–139
25. Maybeck PS (1979) Stochastic models, estimation and control[J], vol 1. Academic Press, Inc., Cambridge, pp 1–16
26. Goad CC, Chadwell CD (1993) Investigation for improving GPS orbits using a discrete sequential estimator and stochastic models of selected physical processes[R]. Goddard Space Flight Center, Greenbelt, p 42
27. Huber PJ (1964) Robust estimation of a location parameter[J]. Ann Math Stat 35(1):73–101
28. Huber PJ (2011) Robust statistics[J]. J Am Stat Assoc 78(381):1248–1251
29. Yamada T, Ando M, Tadokoro K et al (2002) Error evaluation in acoustic positioning of a single transponder for seafloor crustal deformation measurements[J]. Earth Planets Space 54(9):871–882

Publisher's Note Springer Nature remains neutral with regard to jurisdictional claims in published maps and institutional affiliations.